High Impedance Fault Detection and Location Based on Electromagnetic Transient Analysis

W. C. Santos, F. V. Lopes, N. S. D. Brito, B. A. Souza, D. Fernandes Jr., W. L. A. Neves,

***Abstract*—This paper presents HIF detection and location methods for distribution systems, both based on the analysis of HIF-induced electromagnetic transients in strategic points of the distribution network. In order to extract high frequency components from the monitored signals, the discrete wavelet transform (DWT) is used. The wavelet coefficient energies are calculated by sensors installed at various points along the distribution system and, then, used to detect and locate the HIF. The proposed methodology is evaluated by means of Electromagnetic Transients Program (EMTP) simulations of HIFs in a 13.8 kV system, which was modeled from an actual Brazilian distribution network data. Obtained results show that the method is able to distinguish HIFs from other disturbances as well as to provide a significant reduction of the fault search field.**

***Keywords*: Distribution networks, electromagnetic transients, fault detection, fault location, high impedance faults, power systems, smart grids, ATP, wavelet transform.**

I. Introduction

AMONG the many disturbances that the electric power systems are subject, faults (short-circuits) are undoubtedly the most worrisome. In the case of distribution systems, a special class of faults called high impedance faults (HIFs) is cause for concern, especially in overhead distribution networks (DNs) [1], [2].

A HIF occurs when an energized conductor of the primary network makes an electrical contact with a surface of high resistive value, resulting in overcurrents insufficient to sensitize the protection system. As a result, the fault is not cleared, exposing the population to the risk of electric shock and compromising the integrity of the system equipment and of private devices. In this context, the implementation of fast and reliable techniques able to detect and locate HIFs is increasingly becoming an issue of interest for electric utilities.

Several techniques for diagnosing faults on soils with high impedance are available in the literature, as those based on voltage imbalances [3], on the theory of traveling waves [4], and on unconventional algorithms such as artificial neural networks (ANN) [5] and wavelet transform [6]–[9]. Nevertheless, the HIF detection and location are still considered a challenge for protection engineers, what boosted various researches in the area of disturbance diagnosis for DNs.

With the advent of Smart Grids, new concepts in the operation of electrical power systems have become popular, such as the use of sensor networks and the automatic recovering of distribution feeders [10]. In this new scenario, more sophisticated techniques in the protection area has been allowed and, consequently, several HIF detection and location methods have been proposed over the last decades.

From the literature, it is known that the intermittent permanence of the wire on the contact surface during a HIF cause the appearance of high frequency electromagnetic transients between 2 and 10 kHz [6], which may be used for detecting and locating them. This paper presents HIF detection and location methods for distribution systems, both based on the analysis of HIF-induced electromagnetic transients in strategic points of the DN, which are extracted from the monitored signals through the discrete wavelet transform (DWT).

The performance of the proposed method is evaluated through simulated record data obtained from Alternative Transient Program (ATP) [11] simulations of HIFs in a 13.8 kV DN. For this end, a HIF model with two series time-varying resistances controlled by the Transient Analysis of Control Systems (TACS) is applied [12]. Results show that the proposed approach is able to provide a very fast HIF detection and a great defect search field restriction, being suitable for smart grids in which several monitoring points are available.

II. High Impedance Fault Features

According to [2], HIFs generally cause the appearance of electric arcs, what leads to some fault current peculiarities that are following described:

- *Asymmetry*: The fault current has different absolute values for positive and negative half cycle;
- *Nonlinearity*: The voltage-current characteristic curve is nonlinear;
- *Buildup*: The current magnitude increases gradually to its maximum value;
- *Shoulder*: Buildup is ceased for few cycles;
- *Intermittence*: Some cycles in which the energized wire interrupts the contact with the soil.

In Fig. 1 is shown an example of a HIF field test record. One can observe that nonlinearities and asymmetries occur in the whole signal. On the other hand, the intermittence show up

This work was supported by the Brazilian National Research Council (CNPq) and by the Brazilian Coordination for Improvement of Higher Education Personnel (CAPES).

W. C. Santos and F. V. Lopes are Ph.D. students at Federal University of Campina Grande (UFCG), 882 Aprígio Veloso Av., Bodocongó, 58.429-900, Campina Grande, PB, Brazil (e-mail: wellinsilvio.costa@ee.ufcg.edu.br; felipe.lopes@ee.ufcg.edu.br).

N. S. D. Brito, B. A. Souza, D. Fernandes Jr., and W. L. A. Neves are with the Department of Electrical Engineering of Federal University of Campina Grande (UFCG) (e-mail: nubia@dee.ufcg.edu.br; benemar@dee.ufcg.edu.br; damasio@dee.ufcg.edu.br; waneves@dee.ufcg.edu.br).

Paper submitted to the International Conference on Power Systems Transients (IPST2013) in Vancouver, Canada July 18-20, 2013.

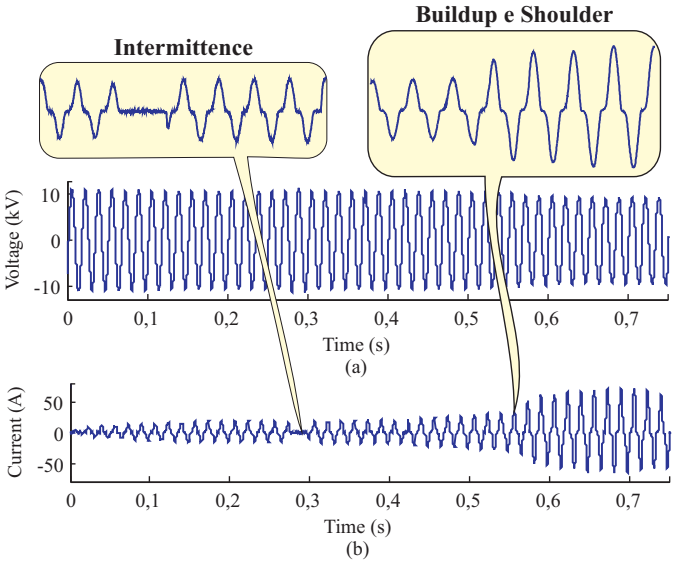

Fig. 1. An actual HIF oscillographic record: (a) voltage; (b) current.

around 0.3 s, whereas both buildup and shoulder occur around 0.55 s. HIFs also generate electromagnetic transients between 2 and 10 kHz due to the intermittent permanence of the wire on the contact surface [6]. Moreover, often the HIF current level is very similar to that observed at steady-state, what can lead conventional overcurrent-based techniques to misoperate, compromising the fault clearing and its locating.

III. Proposed Method

The proposed method is based on the analysis of high frequency components generated by HIFs. These transients are extracted here using the DWT such as following described.

A. The Discrete Wavelet Transform

The DWT is a powerful time-frequency signal-processing tool which allows the analysis of sampled signals with localized transients. In recent decades, such transform has been widely applied to power system problems in the area of transient analysis [13].

Basically, the DWT divides the frequency-band of the input signal into low- and high-frequency components, which are called here as approximation (c) and detail (d) coefficients, respectively. Such components are normally obtained by low- and high-pass filters ($h(k)$ and $g(k)$, respectively) in cascade with down-samplers whose grade is of 2 ($\downarrow 2$). Fig. 2 illustrates the structure of a two-level DWT algorithm applied to an input signal $s(k)$ sampled at a rate of f_s Hz[1].

It is important to point out that the coefficients of both $h(k)$ and $g(k)$ filters depend on the selected mother wavelet. In this work, it is used the Daubechies 4 (db4), which is a mother wavelet quite suitable for detection of fast transients such as those induced by HIF [6], [14].

[1]According to the Nyquist theorem, for a continuous-time waveform sampled at a rate of f_s, the maximum frequency that can be represented by the digital signal is of $f_s/2$ Hz.

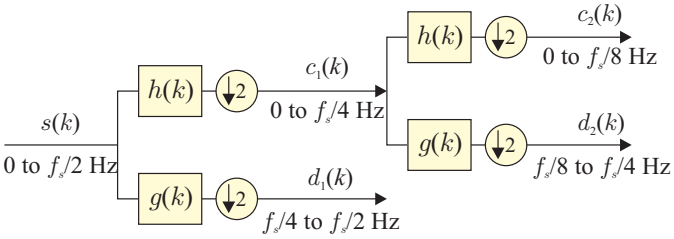

Fig. 2. Structure of two-level DWT algorithm.

B. Energy of HIF-induced Transient

Several fault diagnosis techniques use the detail coefficients to detect monitored signal high frequency components which arise due to faults. However, electrical noises may pose a difficult for such methods, since they can be mistakenly confused with fault-induced transients. This problem is further worrisome for the HIF case, where voltage and current induced transients are commonly attenuated [15].

To overcome the electrical noise problem, the energy spectrum of detail coefficients d — here refereed as ξ — is normally used [13], [14]. According to [14], the computation of the energy ξ at a scale j may be successfully performed using a moving data window that goes through d samples, shifting one coefficient at a time such as follows:

$$\xi_j(k) = \sum_{n=k}^{k+\frac{\Delta k_{cycle}}{2^j}} d_j^2(n) \ , \qquad (1)$$

where Δk_{cycle} is the number of samples in one power frequency cycle of the input signal.

Aiming the reduction of the algorithm computational burden, only detail coefficients at the first scale ($j = 1$) are analyzed here, i.e., ξ is computed using only detail coefficients d_1. Fig. 3 depicts an example of a HIF detection field test case using ξ of voltages (ξ_v) and currents (ξ_i). The oscillographic records were obtained from a Brazilian 13.8 kV DN.

One can see that the HIF beginning time is unclear in both presented voltage and current records, whereas the energies ξ permit the detection of the moment in which fault-induced transients begin at the monitored terminal through the fast-risings in energies ξ_v and ξ_i. Also, it may be noticed that ξ_v assumes greater values than ξ_i after the disturbance inception, in such way that it seems to be more suitable for detecting HIFs. Hence, the proposed algorithm is implemented in such way that only voltage waveform samples are used.

C. Proposed Method Basic Principle

When a disturbance occurs on transmission lines or DNs, induced voltage and current transients, here refereed as traveling waves (TWs), propagate along the conductors, being continuously attenuated until its complete extinction. Fig. 4 illustrates the propagation of fault-induced TWs along a distribution feeder monitored at buses S and R [16]. Since current waveform samples are not used here, only voltage TWs are depicted in Fig. 4, where V_S and V_R are the voltages at buses S and R and superscripts 'b' and 'f' represent backward and forward TWs, respectively.

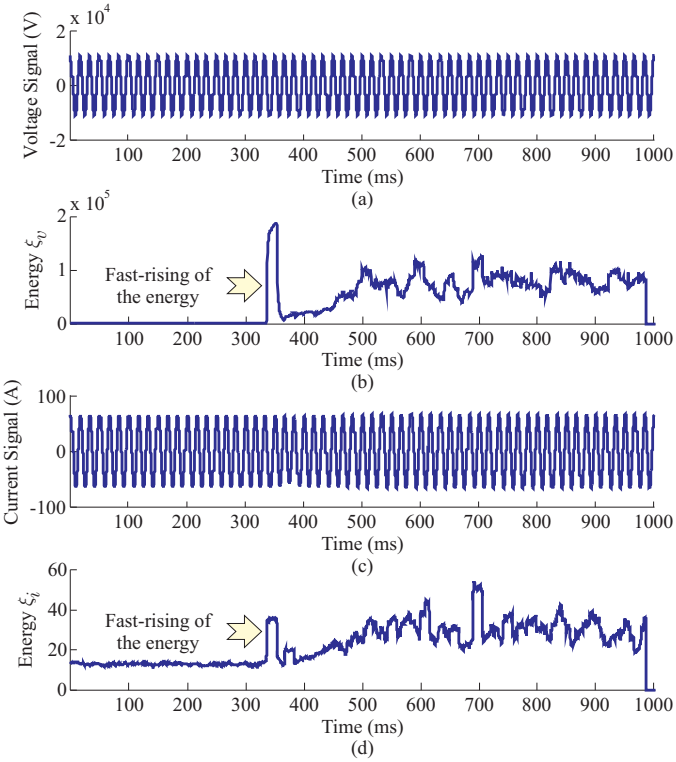

Fig. 3. Example of HIF fault detection: (a) voltage record; (b) detail coefficient of voltages; (c) energy ξ_v; (d) current record; (e) detail coefficient of currents; (f) energy ξ_i.

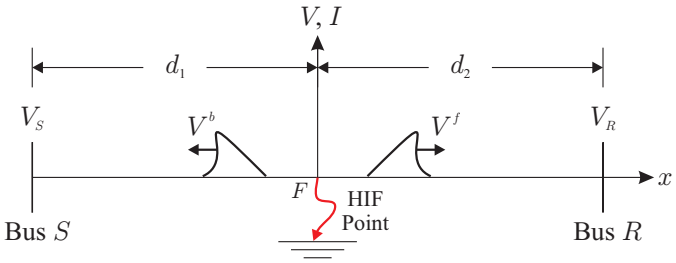

Fig. 4. Faulted branch and the fault induced voltages.

Assuming the fault point F as the reference, it may be seen that both forward and backward fault-induced TWs propagate along the feeder with direction to x and $-x$, so that they may be expressed in the frequency domain as [17]:

$$V(s,x) = V^f(s)e^{-\gamma(s)x} + V^b(s)e^{\gamma(s)x} \ , \tag{2}$$

where $s = j\omega$, ω is the angular dominant frequency of transients and γ is the feeder propagation constant given by:

$$\gamma(s) = \sqrt{(R + j\omega L)\,(G + j\omega C)} \ , \tag{3}$$

where R, L, G and C represent the feeder series resistance, series inductance, shunt conductance and shunt capacitance per unit length, respectively.

Taking into account the propagation of forward and backward TWs from the fault point F (which is located at $x = 0$) until both feeder terminals, one can see that transients into V_S and V_R waveforms can be computed using $x = -d_1$ and $x = d_2$, respectively, so that the transient magnitudes at buses S and R may be estimated using:

$$|V_S(s)| = |V^b(s)e^{-\gamma(s)d_1}| \ , \tag{4}$$

$$|V_R(s)| = |V^f(s)e^{-\gamma(s)d_2}| \ . \tag{5}$$

Substituting the dominant frequency of the the fault-induced transients into (3), the propagation constant can be represented by $\gamma = \alpha + j\beta$, being α and β refereed here as attenuation factor and distortion factor, respectively. Therefore, (4) and (5) can be rewritten as:

$$|V_S(s)| = \left|V^b(s)e^{-(\alpha+j\beta)d_1}\right| = \left|V^b(s)e^{-\alpha d_1}e^{-j\beta d_1}\right| , \tag{6}$$

$$|V_R(s)| = \left|V^f(s)e^{-(\alpha+j\beta)d_2}\right| = \left|V^f(s)e^{-\alpha d_2}e^{-j\beta d_2}\right| . \tag{7}$$

It may be seen that the factors $e^{-\alpha d_1}$ and $e^{-\alpha d_2}$ act adding to the induced TWs an amplitude attenuation, while $e^{-j\beta d_1}$ and $e^{-j\beta d_2}$ introduce an angle displacement. It should be pointed out that sampling rates typically used in DNs commonly blindfold distortions caused by β, since distribution feeders are not so long, i.e., angle displacements are imperceptible in digital voltage and current signals. On the other hand, the comparison of transients magnitude at different points of the power system can provide relevant information regarding the area in which the fault occurred. For instance, if the HIF illustrated in Fig. 4 is closer to the Bus R, $d_1 > d_2 \Rightarrow e^{-\alpha d_1} < e^{-\alpha d_2}$, so that transients are more attenuated at Bus S. Consequently, though it is impossible to estimate the exact fault point using this information, it may be conclude that the search for the defect should preferably start from the Bus R. If other monitored buses are taken into account, one can determine points along the distribution feeder which are near to the fault point, what leads to the reduction of the HIF search field.

In this work, the analysis of transient magnitude is performed through the voltage energy ξ_v computed at strategic points of the monitored DN, in such way that as closer is the fault to the measurement point, greater the transient levels and, consequently, greater the energy ξ_v. This is the theoretical basis of the proposed approach for locating HIFs in smart DNs.

D. HIF Detection

The HIF detection algorithm used here is based on the identification of fast-rising energies into ξ waveforms. As depicted in Fig. 3, such energies are almost constant during the steady-state and increase very fast at the disturbance inception.

In some situations, as in the case of the presence of noises in voltage/current measurements, oscillations in ξ may show up even during the steady-state. Hence, in order to properly detect HIF-induced transients, the hard thresholding procedure is applied here, in which energies smaller than a given threshold are discarded whereas, otherwise, transients are detected. This filtering procedure usually adopts in its formulation the maximum value of the signal used for the transient detection [18]. However, aiming real-time applications for smart grids,

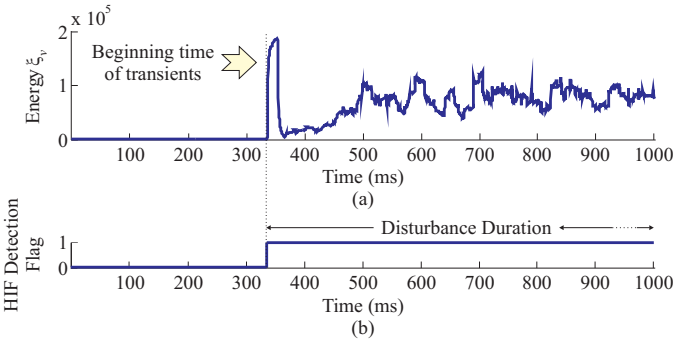

Fig. 5. HIF fault detection: (a) Energy ξ_v; (b) Transient detection flag.

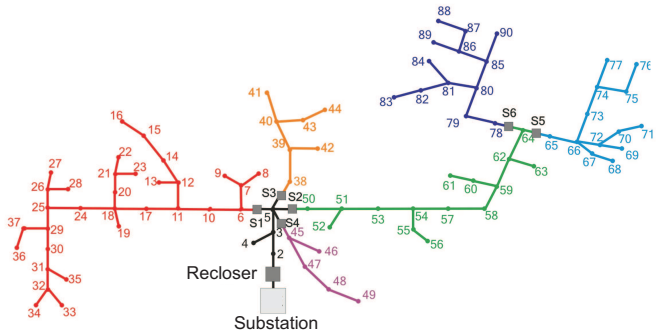

Fig. 6. Modeled 90 bus feeder.

the threshold ρ used here is adjusted through the evaluation of steady-state energies, being given by:

$$\rho = (1 + \eta) \cdot \max\{\xi_{past}\} \ , \tag{8}$$

where ξ_{past} is the set of energy samples in the power frequency cycle that precedes the monitored sample, $\max\{\}$ is a function to compute the global maximum value among analyzed energy samples and η is a secure margin. In [18], the threshold is adopted as 10% of the global maximum of detail-wavelet coefficients, so that the secure margin η used in the proposed approach is taken as 0.1.

In Fig. 5 is shown a transient detection example considering the voltage energy ξ_v presented in Fig. 3. One can see that the HIF detection flag changes its status for '1' almost immediately after the disturbance inception, stopping the calculation of the threshold ρ and triggering the HIF location algorithm, which will be described in the next section. It should be highlighted that, since the HIF is not extinguished, ξ_v keeps greater than ρ for several cycles. According to the Brazilian power grid rules, disturbances in transmission systems and DNs must be detected and cleared in a time less than 150 ms [19], [20]. Thus, if $\xi_v > \rho$ 150 ms after the transient detection and reclosers/circuit breakers keep closed, one can conclude that detected transients were probably induced by a HIF. This analysis can be used to distinguish HIFs from other disturbances or switching procedures, in which energies ξ_v usually decreases rapidly after the transient beginning time. Thus, once detected the HIF, the disturbance location step is performed such as described next.

E. HIF Location

As previously discussed, the exact HIF location is still a challenge for the scientific community. The most of techniques proposed so far in the literature require the knowledge of feeder data and are applied off-line in order to take advantages of more sophisticated procedures [13]. Consequently, they are usually inappropriate for on-line applications in smart DNs.

In this work, although the exact fault point is not estimated, a great restriction of the defect search field is achieved by the analysis of the maximum voltage energies ξ_v values at different points of the DN. Basically, once detected TWs, the maximum transient energies at monitored buses are recorded and, then, a triangulation approach with the three most relevant ξ_v values is applied. Obviously, as greater is the number of monitored points, greater is the accuracy of the proposed approach, which is encouraging for smart DNs in which several monitored points and communication links are available.

IV. Tests and Results

A. Simulated Feeder

To evaluate the proposed algorithm, a 13.8 kV DN was modeled in ATP using actual data provided by a Brazilian utility (Fig. 6). In order to facilitate the DN modeling, all branches were assumed to be composed by 4 AWG wires, the feeder was modeled by using line constant distributed-parameters, loads close each other were put together (resulting in a 90 bus feeder) and a constant impedance load model was used, considering a power factor of 0.955.

Aiming to provide a better comprehension of the proposed approach, the modeled DN was divided into seven areas, called here as DN areas, which are represented by different colors in Fig. 6 (black, red, purple, orange, green, blue and cyan). It makes easier the identification of the area indicated by the proposed algorithm that should be inspected after the HIF detection.

It should be pointed out that the sampling rates used during the analog-to-digital conversion of voltage and current signals have a strong influence on transient based fault diagnosis [21]. In fact, the greater the number of samples per cycle, the better the analysis of high frequency components. Owing that, several devices with high sampling rates have been developed over the last years for transient analysis, like the one reported in [22], whose sampling frequency is of about 5 MHz. Even so, in this paper, we considered a typical rate of 256 samples per cycle (15360 Hz), which shown to be sufficient to provide relevant HIF search field restrictions.

B. Applied Disturbances

The evaluation of the proposed approach was carried out by the analysis of different HIF cases in the DN depicted in Fig. 6, assuming that monitoring devices are installed at buses 32, 44, 49, 56, 90 and 76, i.e., one monitored point for each DN area. For this end, phase A-to-ground faults were applied at buses 13 and 19 (red feeder), 51 and 63 (green feeder), 79 (blue feeder), 74 (cyan feeder), 39 (orange feeder) and 47 (purple feeder).

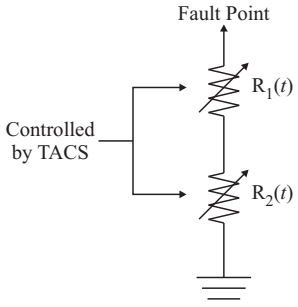

Fig. 8. Model adopted for the HIF.

In this work, the HIF model proposed in [12] was used. It is able to represent the set of characteristics previously illustrated in Fig. 1 like nonlinearity, asymmetry, buildup and shoulder. Basically, two time-varying resistances (R_1 and R_2) controlled by TACS in ATP (Fig. 8) are programmed, in such way that resistance R_1 represents the characteristics of nonlinearity and asymmetry (providing the same characteristics at every cycle of the signal) and resistance R_2 represents the characteristics of buildup and shoulder (just influencing at the beginning of the signal).

C. Simulation Results

In order to illustrate the outputs of the propose algorithm, energies ξ_v and its maximum value are presented for each simulated case in Fig. 7. In all scenarios, the HIF was properly detected at the monitored buses and the maximum transient energy varied with the fault point as desired.

One can see that for the HIFs at the buses 13 and 19, the three maximum values of ξ_v were verified at buses 32, 44 and 49. Performing the proposed triangulation approach, it is concluded that the fault is probably located in the DN areas in red, orange or purple, restricting the fault search field from 90 buses to 44 buses (a reduction of about 51.11%). Similarly, for the HIFs at the buses 39 and 51, the maximum values of ξ_v were detected at buses 44, 49 and 56, indicating that the defect is probably in the feeders in orange, purple and green. So, 27 buses should be inspected instead of 90 buses, leading to a HIF search field restriction of about 70%.

The case of the HIF simulation in bus 63 deserves special attention. This fault caused a considerable energy increase in all buses, but it was unusual the amount of energy detected at the bus 90. The bus 90 is closest to the HIF point than bus 32, for example. This fact shows that it is still necessary a

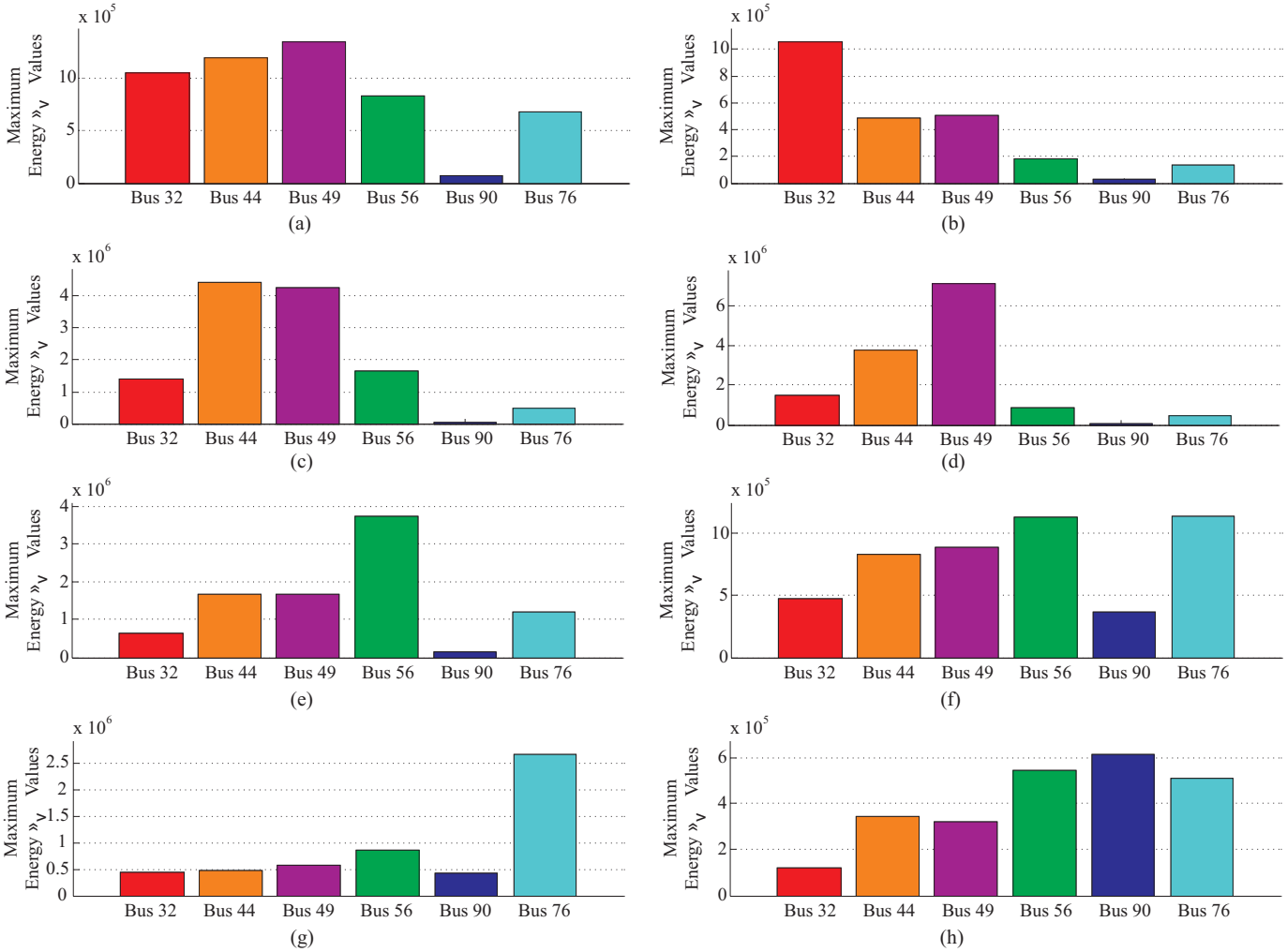

Fig. 7. Maximum transient energies for HIFs at: (a) bus 13; (b) bus 19; (c) bus 39; (d) bus 47; (e) bus 51; (f) bus 63; (g) bus 74; (h) bus 79.

thorough study on the influence of the monitoring point choice, such as its loading, location (middle or end of line) and the number of branches to the possible HIF location.

Similar analyzes to those given may be made for the other cases shown in Fig. 7.

Nevertheless, one can conclude that the proposed method may give support for both off-line and online diagnosing of HIFs in smart DNs with good reliability and generality, since it uses small computational burdens and does not require information regarding the feeder parameters.

V. Conclusions

In this paper a transient based approach aimed at diagnosing HIFs on smart DNs was presented. The technique is based on the theory of TWs since it considers only fault-induced transients to detect the disturbance and then, to identify the area of the monitored smart distribution grid in which the HIF is probably located. For this purpose, the energy spectrum of the discrete wavelet transform detail coefficients is computed in order to analyze signal high frequency components that propagate along the feeders after the fault inception.

Although the method can be applied off-line, it is suitable for real-time smart grid applications, since it does not require information regarding the feeder parameters nor about the power system loads. As a consequence, the proposed algorithm is very simple to be implemented, being applicable in any DN, provided that there are available interconnected monitoring points throughout the system. Basically, the HIF detection step is based on the identification of fast-risings in the energy spectrum of detail-wavelet coefficients while the HIF location approach performs a post-fault processing of the maximum transient energies at strategic areas of the smart grid. Therefore, a reduced area is indicated to be inspected and a search sequence is suggested.

The algorithm was evaluated through ATP simulations of HIF cases in a 13.8 kV DN. For this end, a well-known HIF model available in the literature was implemented. The presented results attest that the proposed method is efficient and quite reliable. In all analyzed scenarios, the HIF was detected and great reductions of the disturbance search field were achieved. Finally, one can conclude that the proposed approach may be easily embedded into smart grid devices in order to provide real-time diagnoses of HIFs in smart DNs.

VI. Acknowledgment

The authors would like to thank the Brazilian National Research Council (CNPq)and the Brazilian Coordination for Improvement of Higher Education Personnel (CAPES) for the financial support of this research.

VII. References

[1] W. Santos, F. Costa, J. Silva, G. Lira, B. Souza, N. Brito, and M. Paes Jr., "Automatic building of a simulated high impedance fault database," in *2010 IEEE/PES Transmission and Distribution Conference and Exposition: Latin America (T&D-LA)*, nov. 2010, pp. 550 –554.

[2] EPRI, "EPRI Report: Detection of Arcing Faults on Distribution Feeders," Palo Alto, Tech. Rep., 1982.

[3] C. V. S. Malagodi, "Sistema de proteção para faltas de alta impedância," Master's thesis, Universidade de São Paulo, São Paulo, SP, 1997.

[4] F. V. Lopes, W. C. Santos, D. Fernandes Jr., W. L. A. Neves, and B. A. Souza, "An adaptive fault location method for smart distribution and transmission grids," in *Innovative Smart Grid Technologies (ISGT Latin America), 2011 IEEE PES Conference on*, oct. 2011, pp. 1 –7.

[5] M.-T. Yang, J.-C. Gu, C.-Y. Jeng, and W.-S. Kao, "Detection of high impedance fault in distribution feeder using wavelet transform and artificial neural networks," in *2004 International Conference on Power System Technology, 2004. PowerCon 2004.*, vol. 1, nov. 2004, pp. 652 – 657 Vol.1.

[6] A.-R. Sedighi, M.-R. Haghifam, O. Malik, and M.-H. Ghassemian, "High impedance fault detection based on wavelet transform and statistical pattern recognition," *Power Delivery, IEEE Transactions on*, vol. 20, no. 4, pp. 2414 – 2421, oct. 2005.

[7] A. Lazkano, J. Ruiz, E. Aramendi, and L. Leturiondo, "A new approach to high impedance fault detection using wavelet packet analysis," in *Ninth International Conference on Harmonics and Quality of Power, 2000. Proceedings.*, vol. 3, 2000, pp. 1005 –1010 vol.3.

[8] H. Mokhtari and R. Aghatehrani, "A new wavelet-based method for detection of high impedance faults," in *International Conference on Future Power Systems, 2005*, nov. 2005, pp. 6 pp. –6.

[9] F. B. Costa, G. R. S. Lira, W. C. Santos, J. A. Silva, B. A. Souza, N. S. D. Brito, and M. R. C. Paes Jr., "High impedance fault detection," in *Internacional Symposium on High Voltage Engineering, 2011. ISH 2011*, Hannover, Germany, Agosto 2011.

[10] S. Massoud Amin and B. Wollenberg, "Toward a smart grid: power delivery for the 21st century," *Power and Energy Magazine, IEEE*, vol. 3, no. 5, pp. 34 – 41, sept.-oct. 2005.

[11] *ATP - Alternative Transient Program*, Leuven EMTP Center, Herverlee, Belgium, 1987.

[12] S. Nam, J. Park, Y. Kang, and T. Kim, "A modeling method of a high impedance fault in a distribution system using two series time-varying resistances in EMTP," in *2001 Power Engineering Society Summer Meeting*, vol. 2, 2001, pp. 1175 –1180 vol.2.

[13] M. M. Saha, J. Izykowski, and E. Rosolowski, *Fault Location on Power Networks*, ser. Power Systems. London: Ed. Springer, 2010.

[14] F. Costa, B. Souza, and N. Brito, "A wavelet-based algorithm to analyze oscillographic data with single and multiple disturbances," in *2008 IEEE Power and Energy Society General Meeting - Conversion and Delivery of Electrical Energy in the 21st Century*, july 2008, pp. 1 –8.

[15] F. V. Lopes, D. Fernandes Jr., and W. L. A. Neves, "Fault location on transmission lines based on travelling waves," *International Conference on Power Systems Transients*, June 2011.

[16] K. R. C. de Oliveira, D. Rodrigo Hartstein Salim, and W. L. A. Neves, "Faulted branch identification on power distribution systems under noisy environment," *International Conference on Power Systems Transients*, June 2009.

[17] A. Greenwood, *Electrical transients in power systems*, Wiley-Interscience, Ed., 1971.

[18] S. Santoso, E. Powers, and W. Grady, "Power quality disturbance data compression using wavelet transform methods," *IEEE Transactions on Power Delivery*, vol. 12, no. 3, pp. 1250 –1257, July 1997.

[19] ONS, *Submódulo 2.6, Requisitos mínimos para os sistemas de proteção e de telecomunicações*, Brasil, 2009.

[20] ANEEL, *Módulo 3 (PRODIST), Acesso ao Sistema de Distribuição*, Brasil, 2008.

[21] W. L. A. Neves, N. S. D. Brito, B. Souza, A. Fontes, K. M. C. Dantas, A. Fernandes, and S. S. B. Silva, "Sampling rate of digital fault recorders influence on fault diagnosis," in *Transmission and Distribution Conference and Exposition: Latin America, 2004 IEEE/PES*, 2004, pp. 406–411.

[22] S. L. Zimath, M. A. F. Ramos, and J. E. S. Filho, "Comparison of impedance and travelling wave fault location using real faults," in *2010 IEEE PES Transmission and Distribution Conference and Exposition*, April 2010, pp. 1 –5.